REPORT NO. HE-150-82

TECHNICAL REPORT

UNIVERSITY OF CALIFORNIA
DEPARTMENT OF ENGINEERING
BERKELEY, CALIFORNIA

INSTITUTE OF ENGINEERING RESEARCH

VISCOUS EFFECTS ON IMPACT PROBES IN A SUBSONIC RAREFIED GAS FLOW

By

E. D. KANE
and
S. A. SCHAAF

SERIES NO. 19

ISSUE NO. 5

DATE MARCH 9, 1951

CONTRACT NAw-5754
REPORT NO. HE-150-82
SERIES NO. 19-5
March 9, 1951

VISCOUS EFFECTS ON IMPACT PROBES IN A SUBSONIC RAREFIED GAS FLOW

By

E. D. KANE
and
S. A. SCHAAF

FACULTY INVESTIGATORS:

R.G. FOLSOM, PROFESSOR OF MECHANICAL ENGINEERING
E.D. KANE, ASSOCIATE PROFESSOR OF ENGINEERING DESIGN
S.A. SCHAAF, ASSISTANT PROFESSOR OF ENGINEERING SCIENCES

Approved by:

NOMENCLATURE

d = diameter of impact probe (in.)

M = Mach number

p = pressure (microns Hg absolute)

p_i = impact pressure

p_1 = static pressure

p_{in} = extrapolated pressure for $1/d = 0$, local reservoir pressure

p_o = reservoir pressure

Re = Reynolds number based on probe diameter

T = temperature (degrees Rankine)

γ = isentropic exponent

μ = coefficient of viscosity (lb/sec.ft)

* * * * * * * * * * * *

VISCOUS EFFECTS ON IMPACT PROBES IN A SUBSONIC RAREFIED GAS FLOW

1.0 INTRODUCTION

The measurement of impact and static pressures in a gas flow has long provided a basic method for determining the Mach number of the stream. At normal pressures, where the Reynolds number based on an impact probe diameter is high, the measured impact pressure is the same as the local reservoir pressure. A simple relation then exists between the Mach number, the static pressure and the measured impact pressure. In a low density gas flow at very low Reynolds numbers, of the order of 100 or less, viscous effects in the flow adjacent to the impact probe become important. The measured impact pressure is no longer the same as the local reservoir pressure but becomes increasingly higher, relatively, as the Reynolds number decreases. Variations will also be observed with respect to static pressures measured with a probe under similar conditions.

The problem of interpreting measured impact pressure has been investigated theoretically and experimentally for incompressible flows in Ref. 1, among others, and experimentally for supersonic flow in Ref. 2. Theoretical results for subsonic compressible flows have been obtained in Refs. 3 and 4. It was the purpose of the investigations described in this report (1) to demonstrate the viscous effect on impact pressure measurements, and (2) to evaluate it by determining experimentally the relation between the measured impact pressure p_i, the local reservoir pressure p_{in}, the Mach M and the Reynolds number Re in subsonic compressible flow.

The tests were performed in a special low pressure subsonic wind tunnel and covered a range of $0.20 < M < 0.45$, $2.5 < Re < 12.5$. The procedure was to place in succession a series of geometrically similar impact probes of different diameter into the same gas flow. For each such run the Mach number was thus fixed while the Reynolds number varied from one probe to another simply by the associated change in diameter. Different impact pressure measurements on the different probes constituted a demonstration of the effect. The evaluation of the effect required a determination of the Mach and Reynolds number in absolute rather than relative terms. This determination was made by an extrapolation process based on the following considerations. Theoretical analyses for compressible flow predict a relation of the form

$$\frac{p_i - p_{in}}{p_{in}} = f(M,Re) \cdot M^2/Re \quad (1)$$

where the form of the function f(M,Re) depends on the nature of the assumptions made, but in all cases varies quite slowly with both Mach and Reynolds number. Since the effect depends on the reciprocal of the Reynolds number, it is observable only at low Reynolds numbers. According to Eq. 1, the measured impact pressures on the series of geometrically similar impact probes of different diameter, d, placed in a fixed stream should vary approximately linearly with 1/d, i.e. 1/Re, a feature which was always observed in the tests. The extrapolated value of such a set of pressures to very large Reynolds number (i.e. 1/d = 0) should correspond to the ideal non-viscous local reservoir pressure. Coupled with a knowledge of the static pressure as obtained at the wall of the wind tunnel nozzle, this extrapolated value was used to determine the Mach and Reynolds numbers of the flow and thus provide a basis for evaluation of the viscous effects. In general terms, the results of the tests were in line with these considerations. However, certain anomalies arose so that the final results must be considered to be of a preliminary nature only. Further work is planned utilizing a larger wind tunnel.

2.0 EQUIPMENT

All test work was performed in the No.2 Wind Tunnel at Berkeley - a continuous operating open-jet type. HYD 2613 is a flow sheet for the wind tunnel and associated equipment (see also PHOTO 198). A detailed description of the unit is given in Ref.5.

2.1 Nozzle

A short subsonic nozzle was employed. The shape of the curved proportion was similar to a standard I.S.A. nozzle (Ref.6), of 3 in. outlet diameter. The length of the constant diameter portion was about one-half the magnitude specified for a standard nozzle. The dimensions are shown on HYD 2612.

2.2 Pumping System

The pumping system of the original installation (Ref.5) was modified by the addition of a Type KB-300 (Distillation Products Inc.) oil jet pump. The pumping system used for this investigation consisted of two KB-300 units backed by a Kinney Type DVD-8810 mechanical pump.

2.3 Pressure Measurements

The reservoir, test section, and nozzle wall pressures could be measured with an oil U-tube manometer (Ref.7) or with a McLeod gage capable of reading a maximum pressure of 250 microns Hg. The McLeod gage was the same basic design as reported in Ref.8, but with the capillary tube and reference volume selected to give a calibration constant of 1.10 mm Hg per cm^2 differential. The least count of the McLeod gage scale is a length of 0.5 mm and estimates are made within this interval using an enlarging lens mounted on the gage frame. Analysis based on a $\pm$ 0.2 mm length reading error shows that the precision of this instrument is $\pm$ 0.2 microns at 25 microns Hg pressure, and $\pm$ 0.6 microns at 250 microns Hg. The oil manometer was used to give a continuous check on the constancy of flow conditions during a run, while all recorded pressures were read on the McLeod gage.

2.4 Probes

Four geometrically similar source-shaped impact probes were constructed for this investigation (HYD 2614 and PHOTO 210). Also a special probe was made identical externally with the 0.450 in. diameter probe (No.1) of HYD 2614, but with an internal baffle added (see HYD 2615). The use of this probe is explained in Section 5.0. The conical probe shown on HYD 2615 and PHOTO 210 was used for static pressure measurements.

2.4 Probes (Continued)

Three test probes could be mounted on the hollow vertical externally-adjustable column during one run. Each probe could be located on the centerline of the nozzle 0.1 in. downstream from the exit plane. The impact pressures reported in Table 1 were made when the impact probes were in this position.

3.0 TESTING PROCEDURE

At the beginning of a group of runs, a pressure check on the equipment was made at no flow through the nozzle. This was done by opening the upstream metering valve until the pressure measured at the nozzle wall increased to the approximate pressure range of the runs. Then the upstream metering valve and the downstream control valve were closed. The system pressure was then read on the McLeod gage through each of the three probes and through the reservoir, nozzle and test section orifices. Any outgassing or leaks in the probe and column system would become apparent and corrections were made before continuing with the run.

The test flow conditions were established. The weight rate of flow was adjusted by means of the upstream metering valve. The pumping speed was varied by throttling with the downstream control valve and by adjusting the power to the KB-300 pumps. The flow rate was observed by a standard Flowrator and by a volumetric flow meter (Ref.5). When the desired flow conditions were attained, pressure readings (three impact probes, reservoir, nozzle wall, test section) were made with the McLeod gage. These readings were repeated to make certain the flow conditions had not shifted. Throughout each run the manometer and flowmeter were frequently checked to watch for instability. In the event that a shift or a periodic flucutation was observed, the run was abandoned and new conditions were set up. At least three minutes was allowed to lapse after taking a reading on the McLeod gage before trapping off for the next one. This delay was considered ample to insure pressure equilibrium, on the basis of available time response data (see Appendix).

The first series of runs were made with probe numbers 1, 2 and 3 mounted on the column. The second series of runs were made with probe numbers 1, 3 and 4 mounted together. The same range of flow conditions were used for both series. The pressure readings obtained with the impact probes are entered in column 5 of Table 1 with the corresponding probe numbers shown in column 2. Several impact and static traverses were made to determine the degree of uniformity of the flow field. The procedure used for pressure measurements when making a traverse of the nozzle was essentially the same as that outlined above. Readings were taken at 0.200 in. intervals across the nozzle 0.1 in. downstream from the exit plane. These traverse data are shown in HYD 2618.

The assumption implicit in the test procedure was that the magnitudes of impact pressures obtained with different probe sizes would be different, although the flow conditions were the same. Provided that the probes were small enough to avoid blocking effects or other disturbances in the upstream nozzle flow, the pressure reading in each case would depend on the Reynolds number of the probe which would vary directly with the probe diameter since flow conditions were constant. An attempt was made to observe blocking effects by measuring the nozzle wall static pressures first with no probe inserted. For every flow condition recorded in this report there was no detectable change in the nozzle wall pressure during this procedure.

4.0 REDUCTION OF DATA

The flow conditions might be deduced from the measured reservoir and nozzle wall static pressures provided the following assumptions are made:

(1) The flow from the reservoir to the test section is isentropic.
(2) The flow is uniform over any cross-section - i.e., the flow is one-dimensional.
(3) The perfect gas law is applicable.

With these assumptions, the Mach number at the test section is related to the measured stagnation pressure p_o and static pressure p_1 by (Ref.9)

$$\frac{p_o}{p_1} = \left(1 + \frac{\gamma - 1}{2} M^2\right)^{\frac{\gamma}{\gamma-1}} \quad \text{-------------} \quad (4.1)$$

The Reynolds number can then be computed from (Ref.10)

$$Re = 2.14 \times 10^{-4} M \, p_1 d / \mu \sqrt{T} \quad \text{---------} \quad (4.2)$$

An alternate technique for determining M involves knowledge of the impact pressure at the test section. If the flow from the reservoir to the test section is adiabatic but non-isentropic, the stagnation pressure measured at the test section, p_{in}, will be lower than that in the reservoir, p_o. Assuming that the deceleration process at the nose of the impact probe is isentropic, then the pressure obtained with the probe will be p_{in}. Stated in another way, the pressure p_{in} will be measured by an impact probe for which the Reynolds number is very large. The impact pressure corresponding to an infinite Reynolds number was estimated for each flow condition in the manner indicated on HYD 2617. The readings of the impact probes for a fixed flow condition were plotted as a function of 1/d, where d is the probe diameter. An infinite Reynolds number would then correspond to the zero value of the abscissa. The open circles on HYD 2617 are the data for one run, while the full circles are the data for a subsequent run at approximately the same flow condition. The points lie on a straight line within the experimental accuracy, indicating a $1/R_e$ dependence for the range of the tests. Extrapolation of the line to the zero value of the abscissa gives a value for p_{in}. The values thus obtained for all runs are listed in column 14 of Table 1. Using these values of p_{in} and the measured static pressures at the nozzle wall, the values of M are computed from Eq. 4.1, with p_o replaced by p_{in}. The Reynolds numbers were computed from Eq. 4.2, using the viscosity data of Ref.11.

5.0 DISCUSSION

Reference to Table 1 shows considerable discrepancy between the measured ratio p_o/p_1 and the calculated ratio p_{in}/p_1. This discrepancy, along with the impact pressure profiles obtained in the nozzle (see HYD 2618) indicates that the flow was non-isentropic. Accordingly, the p_{in}/p_1 data were used in the final computations to determine M (Eq. 4.1). The value p_1, measured at the nozzle wall, was assumed to exist also in the stream. This assumption was checked by traversing the flow at the nozzle exit plane with the conical probe shown on HYD 2615. The pressure distributions are given on HYD 2619, and indicate that the static pressure was very nearly uniform over the flow cross-section and equal to the wall value p_1.

Frequent pressure checks with no flow showed that the maximum error in reading pressures with the McLeod gage - including the effects of McLeod sensitivity, outgassing, ambient temperature changes - did not exceed $\pm \frac{1}{2}$ percent. This figure does not include any systematic errors that might be present, but these are believed to be considerably smaller than $\pm \frac{1}{2}$ percent. This error in the pressures could result in approximately $\pm$ 1 percent in the pressure ratios, or about $1\frac{1}{2}$ percent maximum error in ratios involving p_{in}. Errors of this magnitude are serious in the present tests. For example, at $M = 0.2$, an uncertainty of $\pm 1\frac{1}{2}$ percent in the present ratio used in Eq. 4.1 results in an error of more than $\pm$ 20 percent in M. At the highest M of the present tests ($M = 0.44$), the estimated maximum error in M is $\pm$ 10 percent. These variations in M are present also in Re as calculated from Eq. 4.2.

Homann (Ref.1) gave an analysis for the impact pressures obtained in incompressible viscous flows at the forward stagnation point of a sphere. His results were extended in Ref.4 to include the effect of compressibility and in Ref.3 to include the "slip" effect expected in the rarefied gas dynamics flow regime. These analyses reduce to the form

$$\frac{p_i - p_{in}}{p_1} = (\text{correction factor})\ \frac{M^2}{Re}$$

The correction factor varies from a constant in the case of incompressible flow without slip to various functions of M and Re depending upon the assumptions made. For purposes of comparison with these analyses, the impact pressure correction, $(p_i - p_{in})/p_1$, was computed from the data and is shown on HYD 2620 as a function of the parameter M^2/Re.

Examination of HYD 2620 shows that the correction factor is positive over the range of the data - i.e., an impact probe in a subsonic low density gas flow gives an impact pressure p_i higher than would be computed for a non-viscous flow. This effect is in accord with the predictions of the available theory. HYD 2620 also indicates that a 1 percent error in p_i can be expected for a flow in which M^2/Re is approximately 0.002. The data are not accurate enough to warrant an attempt to distinguish the form of the correction factor as predicted by the various theories. A single curve has been faired through the data of HYD 2620, which might be used for preliminary estimating purposes for flows coming within the range of the experimental variables. The average slope of this curve is 4.5, whereas the theoretical prediction is approximately twice this value.

Referring to HYD 2617, the ratio p_{in}/p_o is greater than 1. This result was obtained for all of the runs, the ratio varying from 1.002 to 1.050. If the extrapolation procedure is correct, and p_{in} represents the true impact pressure of the flow at the test section, then the increase in impact pressure might be explained if the flow from the reservoir to the test section is non-adiabatic. In order to check this possibility, the probe shown on HYD 2615 was constructed with a thermocouple welded to the internal baffle. The probe was inserted in the flow, and a potentiometer was used to determine whether any temperature difference existed between the probe thermocouple and the thermocouple placed in the reservoir of the wind tunnel. The probe temperature was investigated over the entire range of variables covered in these tests, and no rise in the probe baffle temperature was detected, indicating that the flow was adiabatic. However, the question of what minimum change in stagnation temperature could have been detected by the probe was not answered. The probe thermocouple would assume the flow stagnation temperature (or slighter lower under continuum conditions) only if heat transfer radiation and conduction was negligibly small compared to convection from the flowing gas. Since convective heat transfer rates decrease at low gas densities, measurement of convective effects requires special efforts to minimize and evaluate radiation and conduction losses (Ref.12). These precautions were not observed fully during the subject experiment, so that the apparent conclusion regarding adiabaticity of the flow is considered tentative.

Another hypothesis was that the gas density conditions were low enough so that internal flow effects in the probe system, as predicted in Ref.13, might be present. To check this, the probe shown on HYD 2615, with the internal baffle, and probe No.1 of HYD 2614, which were identical externally in every respect, were compared directly by insertion into the same flows. In every case, the two probes gave identical readings, so that the internal flow hypothesis is considered untenable.

In view of these results, the high values of the ratio p_{in}/p_o remain unexplained. Since the magnitude of p_{in} determines the flow conditions, according to Eqs. 1 and 2, the entire basis of attempting correlation of the experimental data is in doubt. The present report, therefore, must be considered preliminary, and an improved experimental technique is required to obtain definitive results.

6.0 CONCLUSIONS

6.1 Source-shaped impact probes placed in subsonic low density gas streams yield impact pressures which are higher than would be predicted from the usual non-viscous theory.

6.2 For the source-shaped probe, for Mach numbers between 0.21 and 0.49 and Reynolds numbers (based on probe diameter and free stream properties) between 2.5 and 12.7, the present results indicate that the non-viscous theory produces an error of 1 percent in impact pressure when the flow parameter Mach number squared over Reynolds number is approximately 0.002. As the parameter increases, the correction increases in the present tests; the correction reached 20 percent when the parameter M^2/Re was approximately 0.05.

6.3 The present results must be considered tentative and of a preliminary nature, in view of unexplained discrepancies in the variables used to specify flow conditions.

-- E.D. KANE
and
S.A. SCHAAF

MARCH 9, 1951

APPENDIX

1.0 OUTGASSING EFFECTS

The problem of time response of pressure gaging systems used with low density flows has been discussed in Ref.14, and the effect of outgassing on pressure magnitudes was indicated in the same reference. Briefly, gases or vapors adhering to the internal walls of the pressure gaging system behave like gas sources and produce a pressure rise in the gage system which has no relation to the external flow. The effect can also occur in the reverse direction, with "in-gassing" or the action of an effective sink in the gage system as gases entering through the probe orifice are adsorbed to the walls. For given surface conditions, the magnitude of the pressure error to be expected due to out-gassing depends on the dimensions of the probe system.

In the present tests, it was desirable to use the smallest possible probe to yield the lowest possible Reynolds number. The lower limit on size was fixed by outgassing effects, evaluated by the following procedure.

2.0 PROCEDURE

The pumping system was adjusted to give a pressure, measured at the reservoir, of 9 microns Hg with no flow into the wind tunnel. The upstream metering valve was then opened and the air flow rate adjusted to give a pressure of 100 microns in the reservoir under steady flow conditions. The pressure read by one of the impact tubes, inserted into the flow, was measured. The upstream metering valve was then closed rapidly, and the reservoir pressure, p_o, and the impact probe pressure, p_i, were measured simultaneously at definite time intervals. Another probe was inserted into the flow and the procedure repeated, until the pressure-time data had been obtained for each probe investigated. The results for a series of tests involving probe Nos.1, 2 and 3 are shown on HYD 2616.

3.0 RESULTS

From HYD 2616, it is clear that the smallest probe (No.3) requires the longest time to reach equilibrium. After a sufficient time has elapsed (about 180 seconds), this probe read the same, within the accuracy of measurement, as the other two.

When a similar experiment was performed utilizing a probe which was one-half the size of probe No.2, it indicated a pressure, after 180 seconds, which was almost 10 microns Hg higher than the other probes. Accordingly, only probe Nos. 1, 2, 3 and 4 were employed in the experiments, and a time of at least 180 seconds was allowed to elapse between a change of setting and the reading of the instruments.

* * * * * * * * *

R E F E R E N C E S

1) F. Homann - "Der Einfluss grosser Zähigkeit bei der Strömung um den Zylinder und um die Kugel", ZAMM, Band 16, Heft 3, Juni 1936, p.153.

2) E.D. Kane and G.J. Maslach - "Impact Pressure Interpretation in a Rarefied Gas at Supersonic Speeds", N.A.C.A. TN 2210, October 1950.

3) T.C. Lin and S.A. Schaaf - "The Effect of Slip on Flow Near a Stagnation Point and in a Boundary Layer", Univ. of Calif. Eng. Projects Report HE-150-76, October 1950.

4) P.L. Chambre - "The Theory of the Impact Tube in a Viscous Compressible Gas", Univ. of Calif. Eng. Projects Report HE-150-50, November 1948.

5) E.D. Kane and D.E. Emerson - "Construction and Operation of a Small Low Density Supersonic Wind Tunnel (No.2 Wind Tunnel)", Univ. of Calif. Eng. Projects Report HE-150-57, March 1949.

6) NACA TM-952 - "Standards for Discharge Measurements with Standardized Nozzles and Orifices".

7) G.J. Maslach - "A Precision Manometer for Low Pressures", Univ. of Calif. Eng. Projects Report HE-150-75, October 1950.

8) F.C. Hurlbut - "Instrumentation for Molecular Beam (3. McLeod Gage Calibration)" Univ. of Calif. Eng. Projects Report HE-150-55, June 1950.

9) H.W. Liepmann and A.E. Puckett - "Aerodynamics of a Compressible Fluid", John Wiley & Sons, Inc., New York, 1947, p.26.

10) E.D. Kane - "Drag Forces on Spheres in Low Density Supersonic Gas Flow", Univ. of Calif. Eng. Projects Report HE-150-65, February 1950.

11) J.H. Keenan and J. Kaye - "Thermodynamic Properties of Air", John Wiley & Sons, Inc., New York, 1945, p.3.

12) R.M. Drake and E.D. Kane - "A Summary of the Present Status of Heat Transfer in Rarefied Gases", Univ. of Calif. Eng. Projects Report HE-150 -73, October 1950.

13) P.L. Chambre and S.A. Schaaf - "The Theory of the Impact Tube at Low Pressures" Jour.Aero.Sci., Vol.15, No.12, December 1948, pp 735-737.

14) S.A. Schaaf and R.R. Cyr - "Time Constants for Vacuum Gage Systems", Jour. Appl. Phys., Vol.20, No.9, September 1949, pp 860-863.

* * * * * * * * * * *

Run	Probe No.	p_o	p_1 (microns Hg)	p_i	p_{in}/p_o	p_o/p_1	p_{in}/p_i	M	T_o (°R)	d (in.)	Re	M^2/Re	p_{in} (mic.Hg)	$\frac{p_i - p_{in}}{p_1}$
40b	1	89.1	87.2	92.4	1.010	1.022	1.032	0.214	540	0.450	6.22	0.00736	90.0	0.0275
	2			93.9						0.300	4.15	0.1103		0.0447
	3			95.3						0.225	3.11	0.0147		0.0608
40d	1	53.6	51.7	59.1	1.024	1.037	1.062	0.294	547	0.450	5.04	0.0172	54.9	0.0812
	2			60.9						0.300	3.36	0.0257		0.116
	3			63.0						0.225	2.52	0.0342		0.157
41a	1	58.4	54.3	66.5	1.050	1.076	1.130	0.421	549	0.450	7.70	0.0230	61.3	0.0958
	2			69.0						0.300	5.13	0.0345		0.142
	3			72.0						0.225	3.85	0.0460		0.197
41b	1	84.3	81.2	90.0	1.020	1.038	1.059	0.288	549	0.450	7.74	0.01072	86.0	0.0493
	2			92.2						0.300	5.16	0.0161		0.0734
	3			94.5						0.225	3.87	0.0214		0.105
43a	1	43.9	40.3	50.1	1.035	1.089	1.127	0.417	526	0.450	6.37	0.0304	45.4	0.1017
	2			51.7						0.300	4.25	0.0456		0.141
	3			54.0						0.225	3.19	0.0608		0.200
43c	1	95.8	92.2	101.8	1.015	1.039	1.055	0.277	541	0.450	8.54	0.0089	97.2	0.0499
	2									0.300	5.69	0.0135		0.0748
	3									0.225	4.27	0.0179		0.101
43d	1	137.0	134.5	142.0	1.014	1.019	1.033	0.215	542	0.450	9.60	0.00482	139.0	0.0223
	2			144.0						0.300	6.40	0.00722		0.0372
	3			145.5						0.225	4.80	0.00964		0.0483
40b'	1	89.9	88.1	92.4	1.002	1.020	1.022	0.174	537	0.600	6.83	0.00443	90.1	0.0261
	2			93.2						0.450	5.13	0.00592		0.0352
	3			96.4						0.225	2.56	0.0118		0.0715
40d'	1	54.8	52.6	59.1	1.023	1.042	1.066	0.302	543	0.600	7.09	0.0128	56.1	0.0570
	2			60.1						0.450	5.31	0.0172		0.0760
	3			63.9						0.225	2.66	0.0344		0.148
41a'	1	59.3	55.0	65.5	1.050	1.078	1.132	0.423	543	0.600	10.63	0.0168	62.3	0.0582
	2			67.5						0.450	7.97	0.0224		0.0945
	3			72.2						0.225	3.99	0.0448		0.180
41b'	1	83.7	80.5	88.1	1.020	1.040	1.061	0.291	542	0.600	10.45	0.00810	85.4	0.0335
	2			89.9						0.450	7.83	0.01081		0.0559
	3			94.1						0.225	3.92	0.0216		0.108
43a'	4	42.6	39.8	47.4	1.042	1.070	1.118	0.402	542	0.600	7.28	0.0222	44.5	0.0728
	1			48.5						0.450	5.46	0.0295		0.1005
	3			52.5						0.225	2.73	0.0592		0.201
43b'	4	69.9	64.2	76.2	1.035	1.089	1.127	0.417	528	0.600	12.68	0.0137	72.3	0.0607
	1			78.0						0.450	9.51	0.0183		0.0888
	3			83.5						0.225	4.76	0.0365		0.174

T A B L E I.

TABLE I. (CONTINUED)

Run	Probe No.	p_o	p_1 (microns Hg)	p_i	p_{in}/p_o	p_o/p_1	p_{in}/p_i	M	T_o (°R)	d (in.)	Re	M^2/Re	p_{in} (mic.Hg)	$\frac{p_i - p_{in}}{p_1}$
43c	4	96.5	98.0	101.5	1.015	1.038	1.054	0.274	541	0.600	11.36	0.00661	97.9	0.0387
	1			103.0							8.52	0.00881		0.0548
	3			107.5							4.26	0.0176		0.1032
43d	4	138.0	135.0	141.5	1.008	1.022	1.030	0.205	543	0.600	12.25	0.00343	139.0	0.0185
	1			142.5						0.450	9.19	0.00457		0.0259
	3			146.0						0.225	4.59	0.00916		0.0519

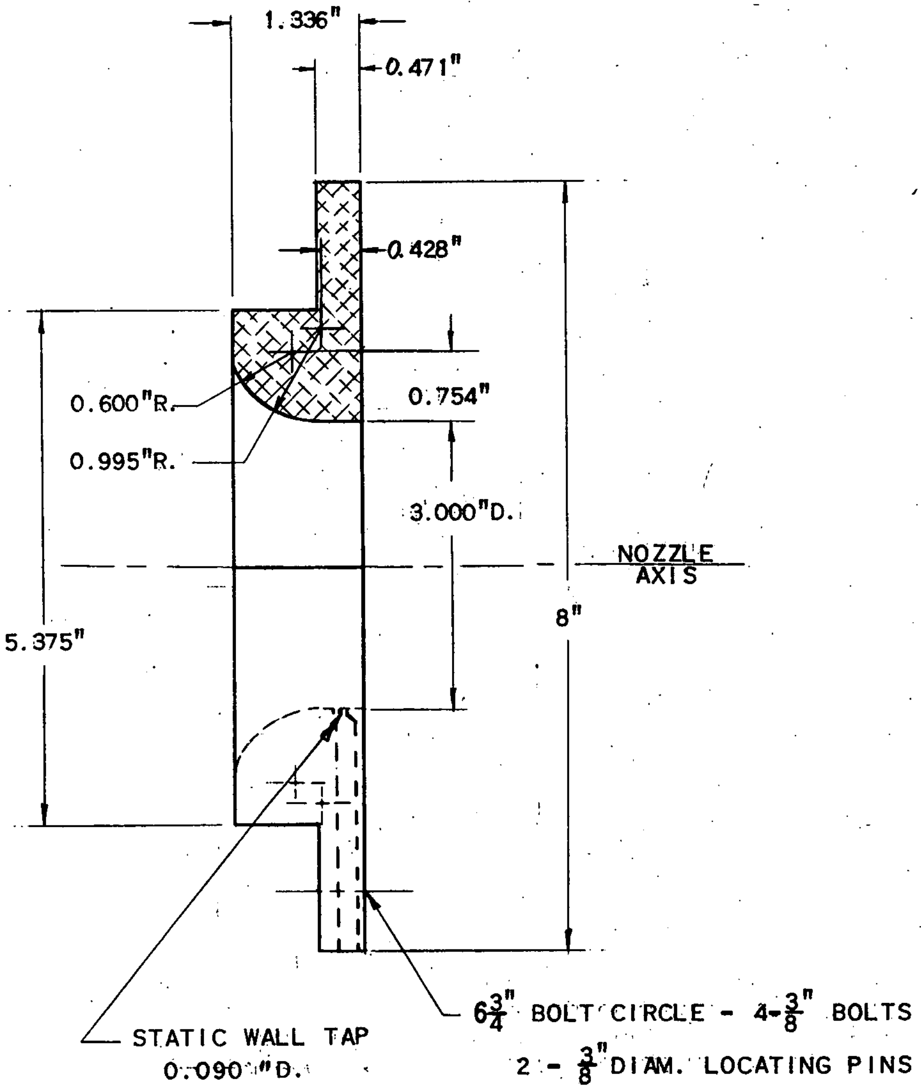

3 INCH NOZZLE

HYD-2612-150-0

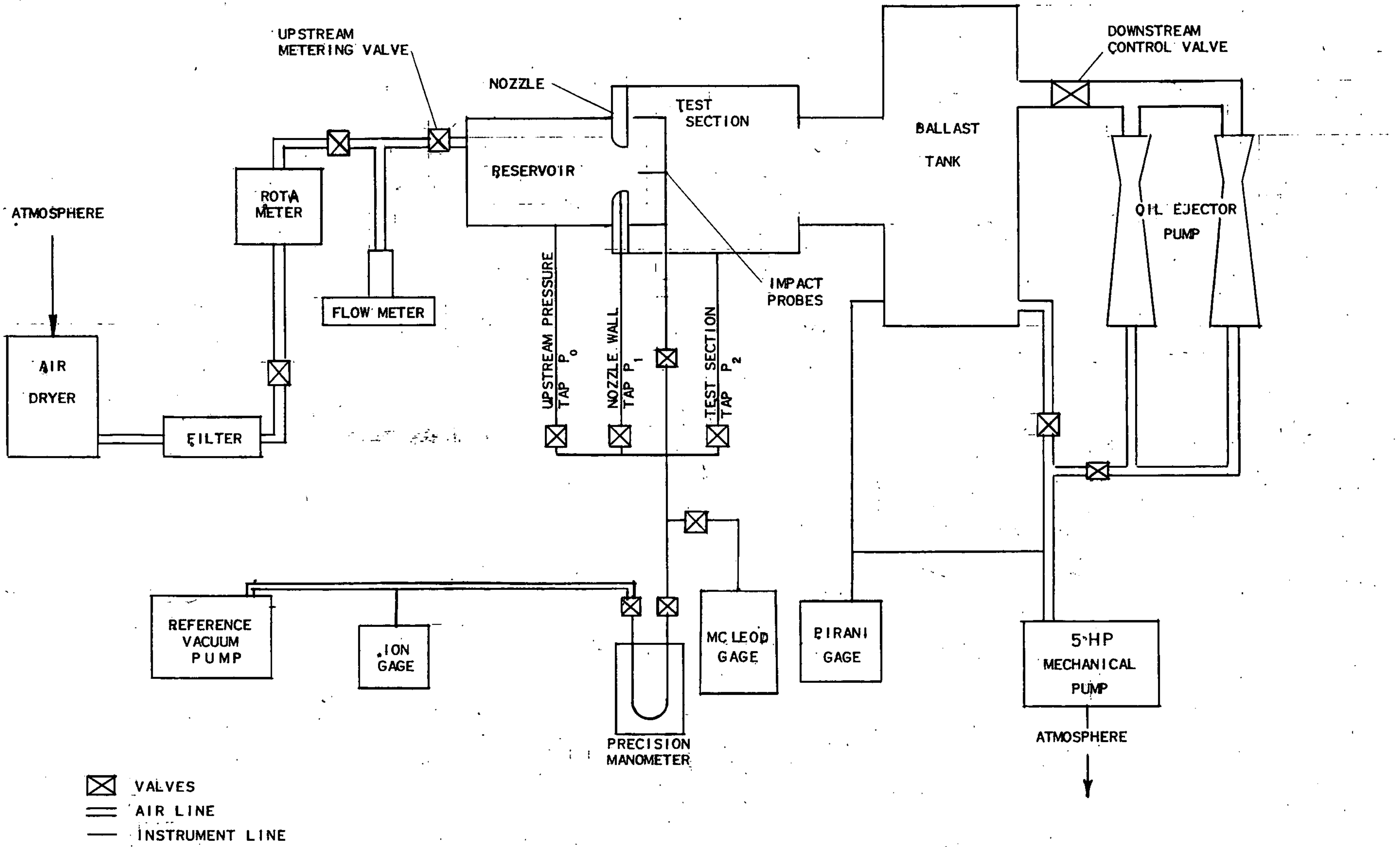

SCHEMATIC OF NUMBER 2 WIND TUNNEL

HYD 2613-150-0

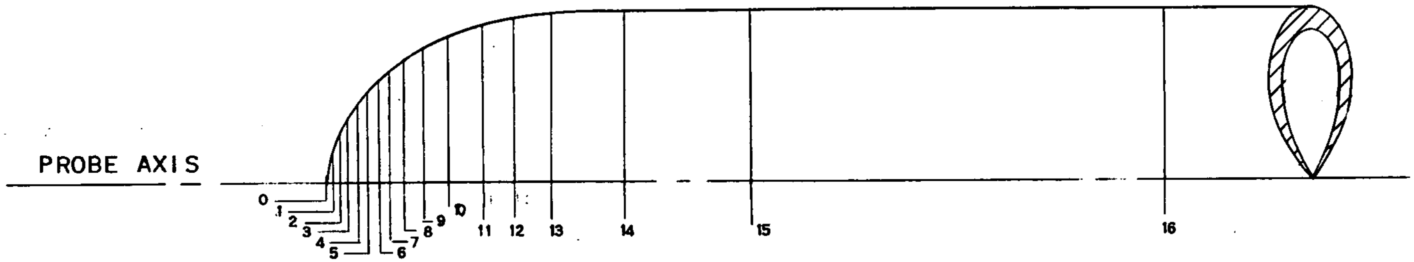

STATION	PROBE 1 0.450" TUBE OUTSIDE DIAM. 0.090" ORIFICE DIAM.		PROBE 2 0.300" TUBE OUTSIDE DIAM. 0.060" ORIFICE DIAM.		PROBE 3 0.225" TUBE OUTSIDE DIAM. 0.045" ORIFICE DIAM.		PROBE 4 0.600" TUBE OUTSIDE DIAM. 0.120" ORIFICE DIAM.	
	AXIAL DISTANCE	OFFSET	AXIAL DISTANCE	OFFSET	AXIAL DISTANCE	OFFSET	AXIAL DISTANCE	OFFSET
0	0.0000	0.0000	0.0000	0.0000	0.0000	0.0000	0.0000	0.0000
1	0.0081	0.0489	0.0054	0.0325	0.0040	0.0245	0.0108	0.0650
2	0.0114	0.0585	0.0076	0.0389	0.0057	0.0292	0.0152	0.0778
3	0.0210	0.0771	0.0139	0.0513	0.0105	0.0385	0.0278	0.1026
4	0.0330	0.0951	0.0219	0.0634	0.0165	0.0475	0.0438	0.1268
5	0.0477	0.1125	0.0317	0.0750	0.0238	0.0562	0.0634	0.1500
6	0.0657	0.1290	0.0437	0.0860	0.0328	0.0645	0.0874	0.1720
7	0.0870	0.1446	0.0580	0.0964	0.0435	0.0723	0.1160	0.1928
8	0.1125	0.1593	0.0750	0.1061	0.0562	0.0796	0.1500	0.2122
9	0.1431	0.1725	0.0953	0.1149	0.0715	0.0862	0.1906	0.2298
10	0.1797	0.1845	0.1197	0.1229	0.0898	0.0922	0.2394	0.2458
11	0.2250	0.1950	0.1500	0.1299	0.1125	0.0975	0.3000	0.2598
12	0.2838	0.2040	0.1891	0.1359	0.1419	0.1020	0.3782	0.2718
13	0.3645	0.2115	0.2429	0.1410	0.1822	0.1057	0.4845	0.2820
14	0.4890	0.2175	0.3260	0.1449	0.2445	0.1087	0.6520	0.2898
15	0.7212	0.2217	0.4808	0.1477	0.3606	0.1108	0.9616	0.2954
16	1.3836	0.2241	0.9224	0.1494	0.6918	0.1120	1.8448	0.2988

NOTE: ORIFICE IS BORED AFTER TUBE IS MACHINED TO ABOVE DIMENSIONS.

PROFILE DIMENSIONS FOR SOURCE SHAPED IMPACT PROBES.

HYD 2614-150-0

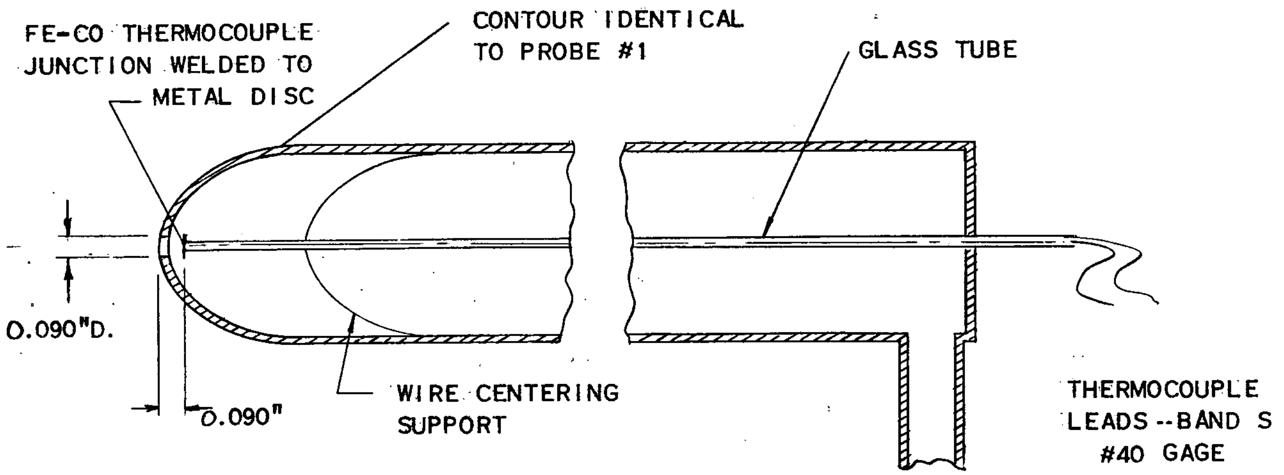

No. I PROBE WITH INTERNAL BAFFLE

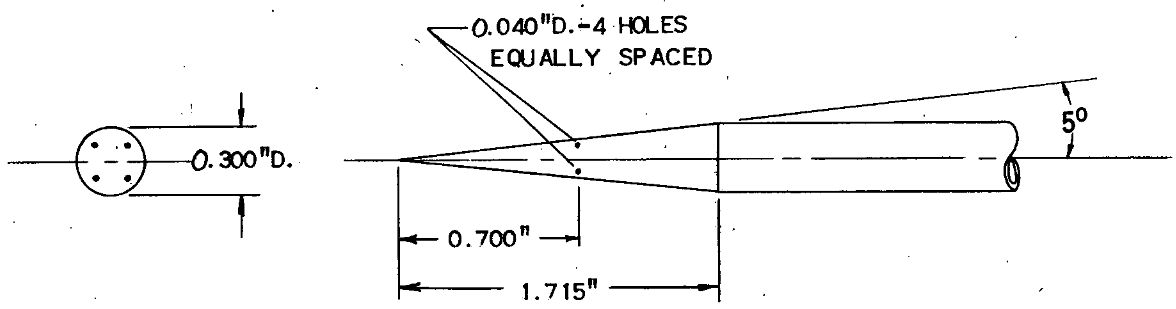

STATIC PRESSURE PROBE

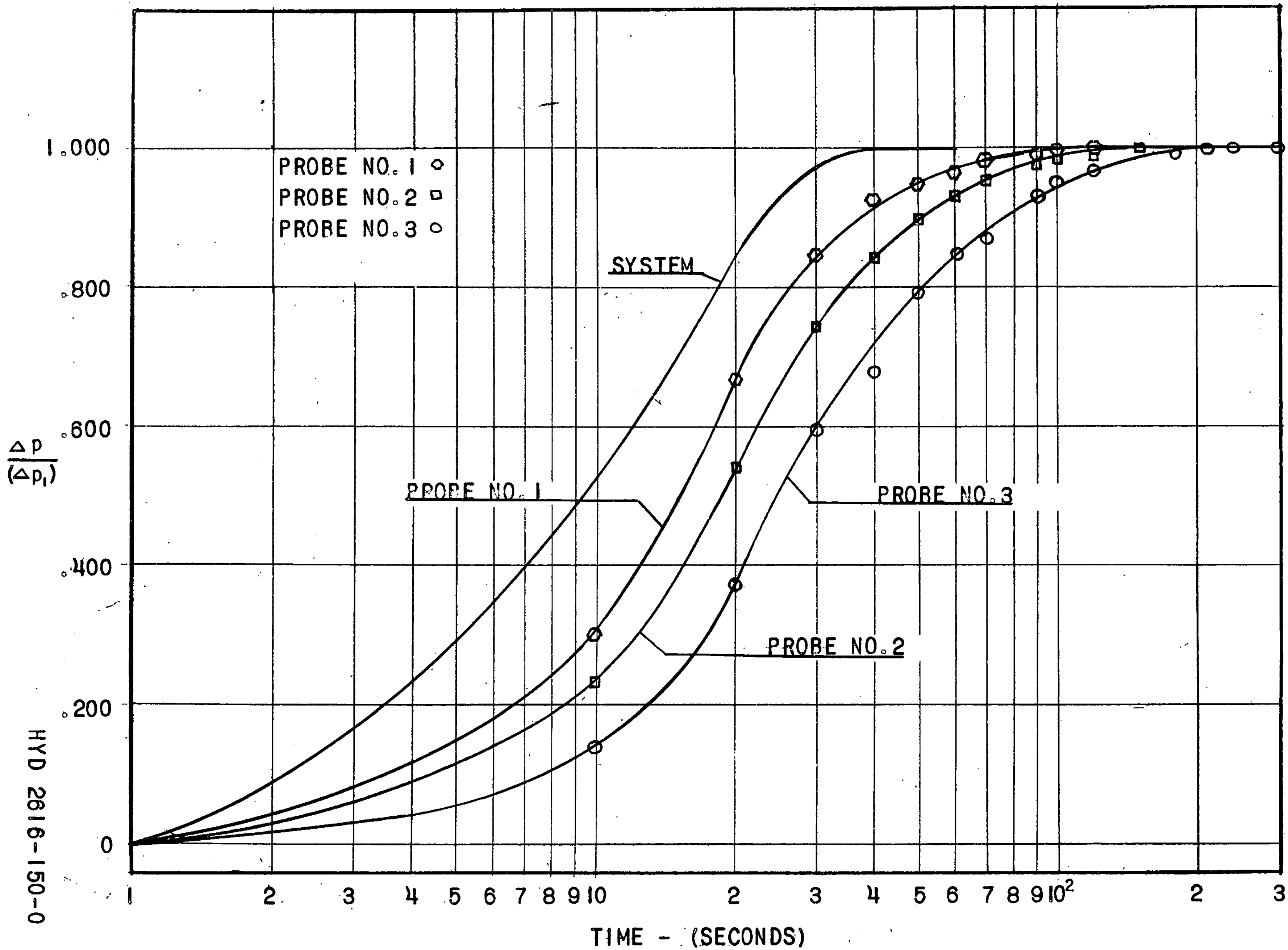

HYD 2616-150-0

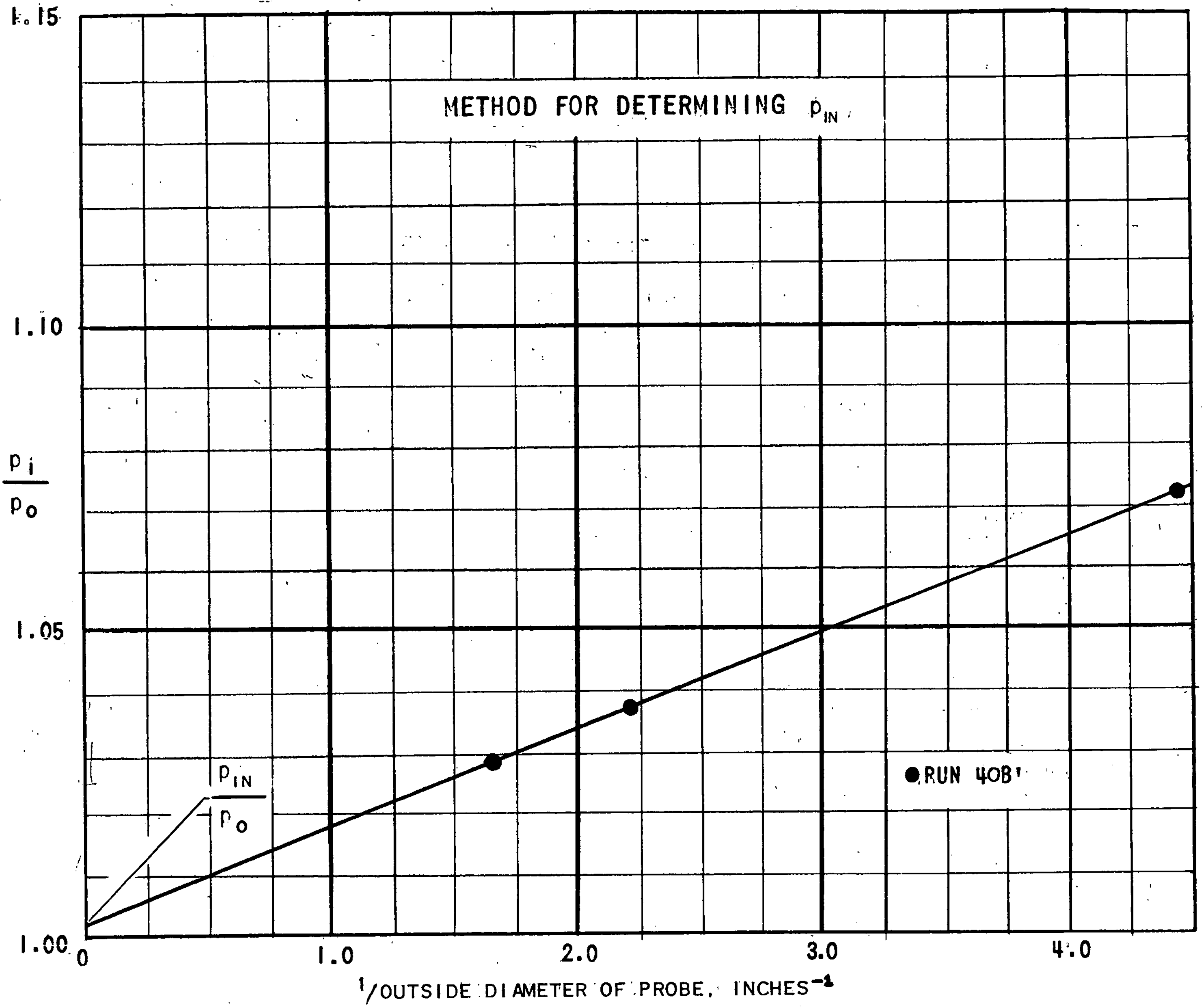

HYD 2617-150-0

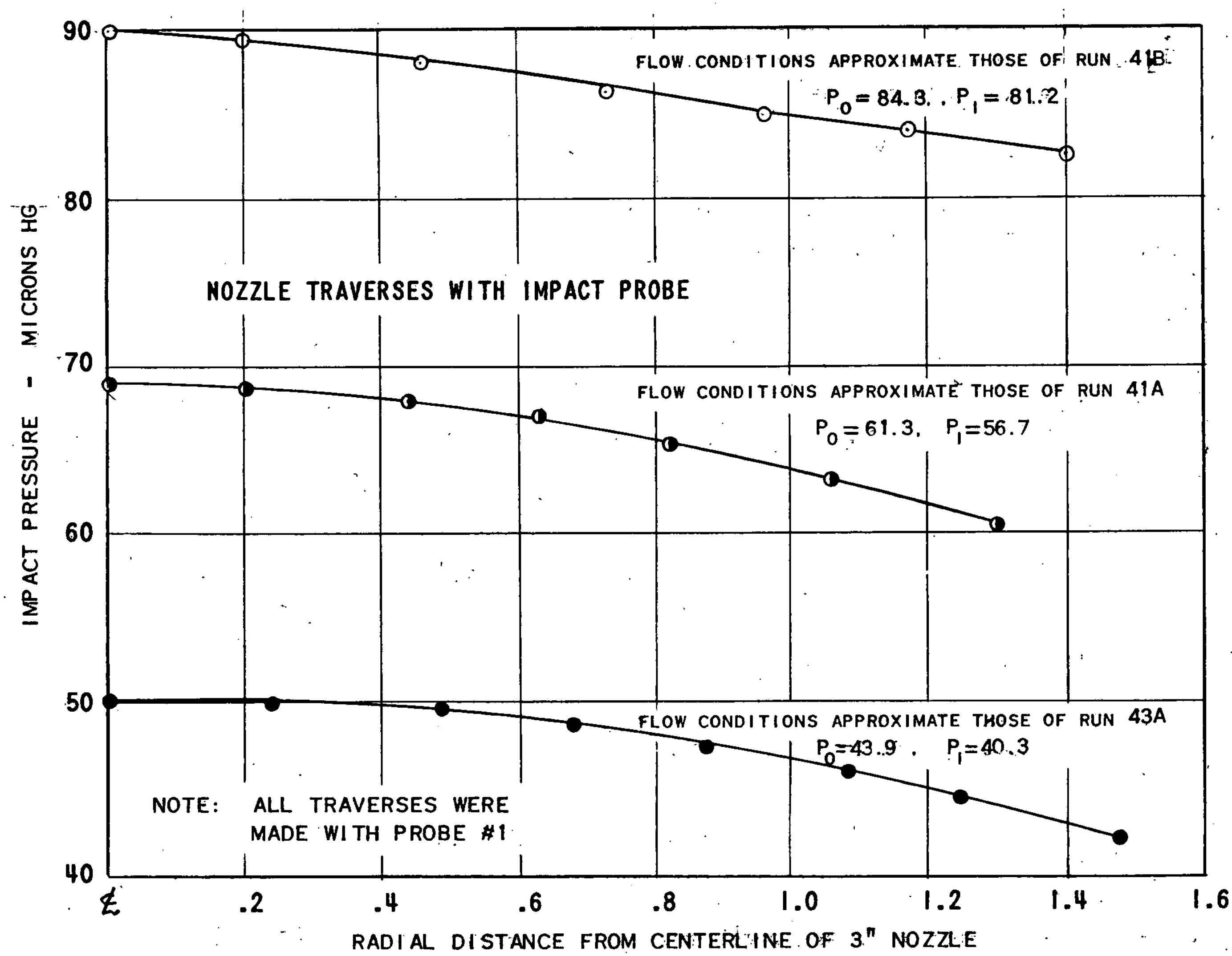

HYD 2618-150-0

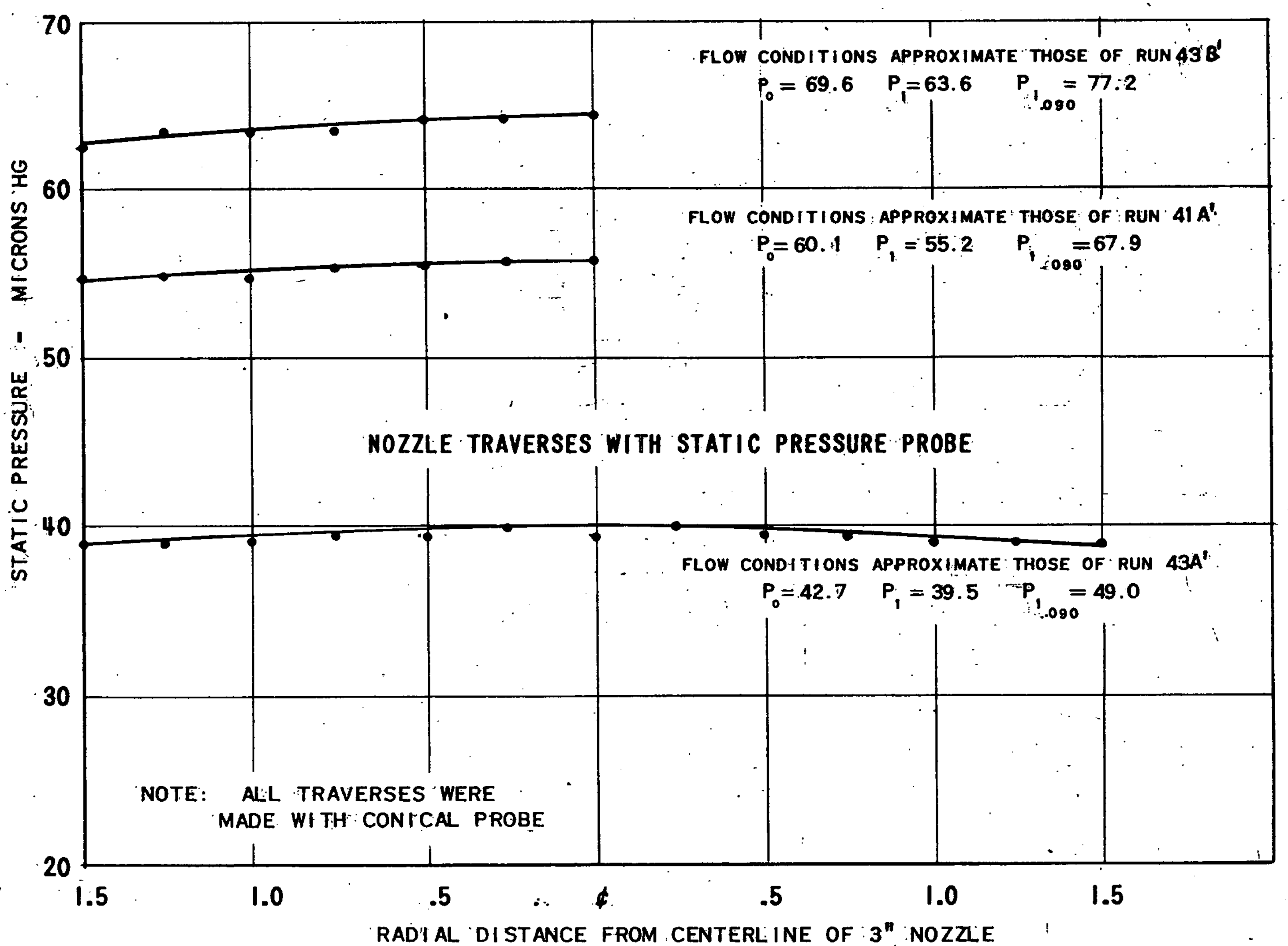

HYD 2619-150-0

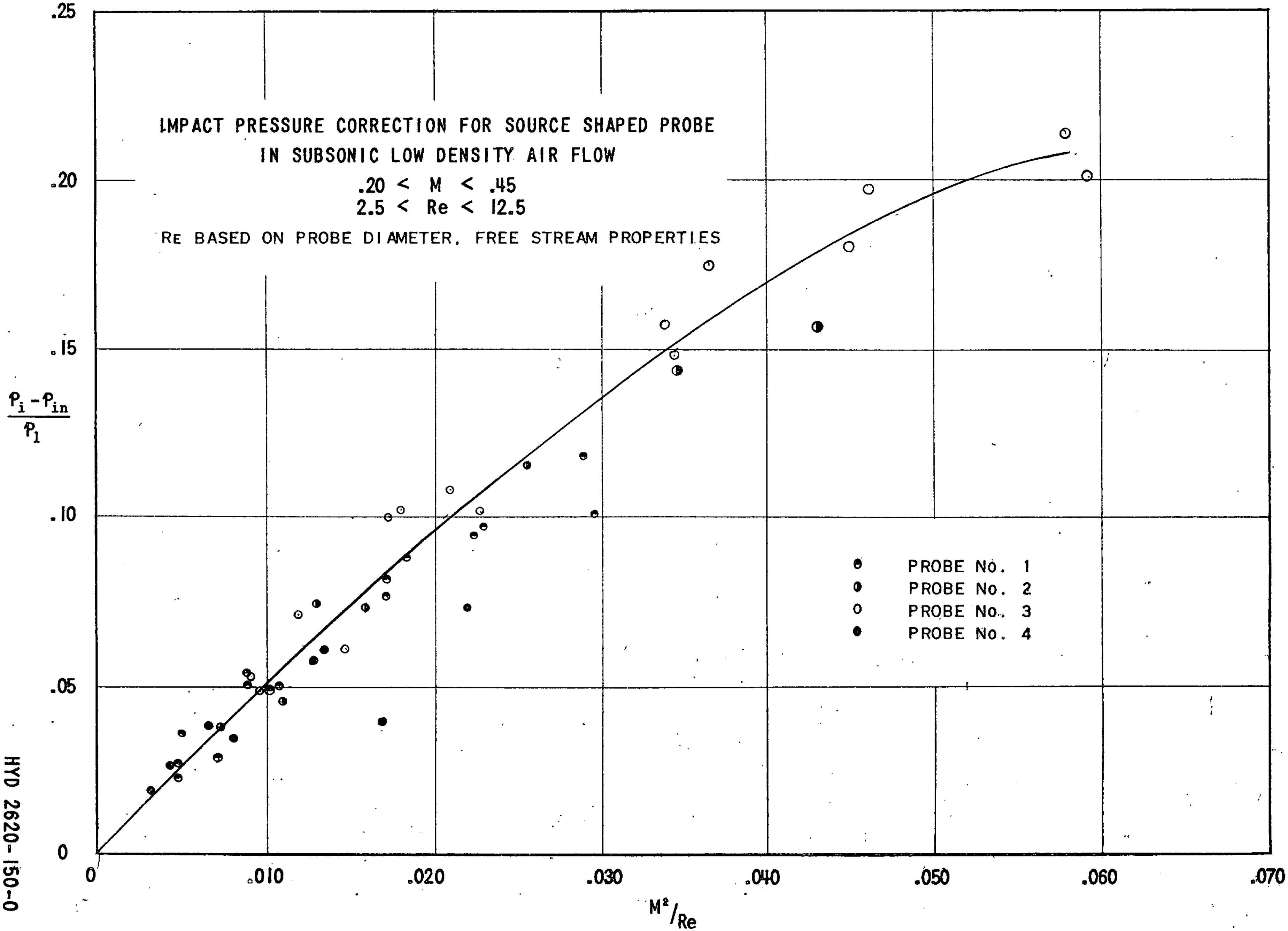

HYD 2620-150-0

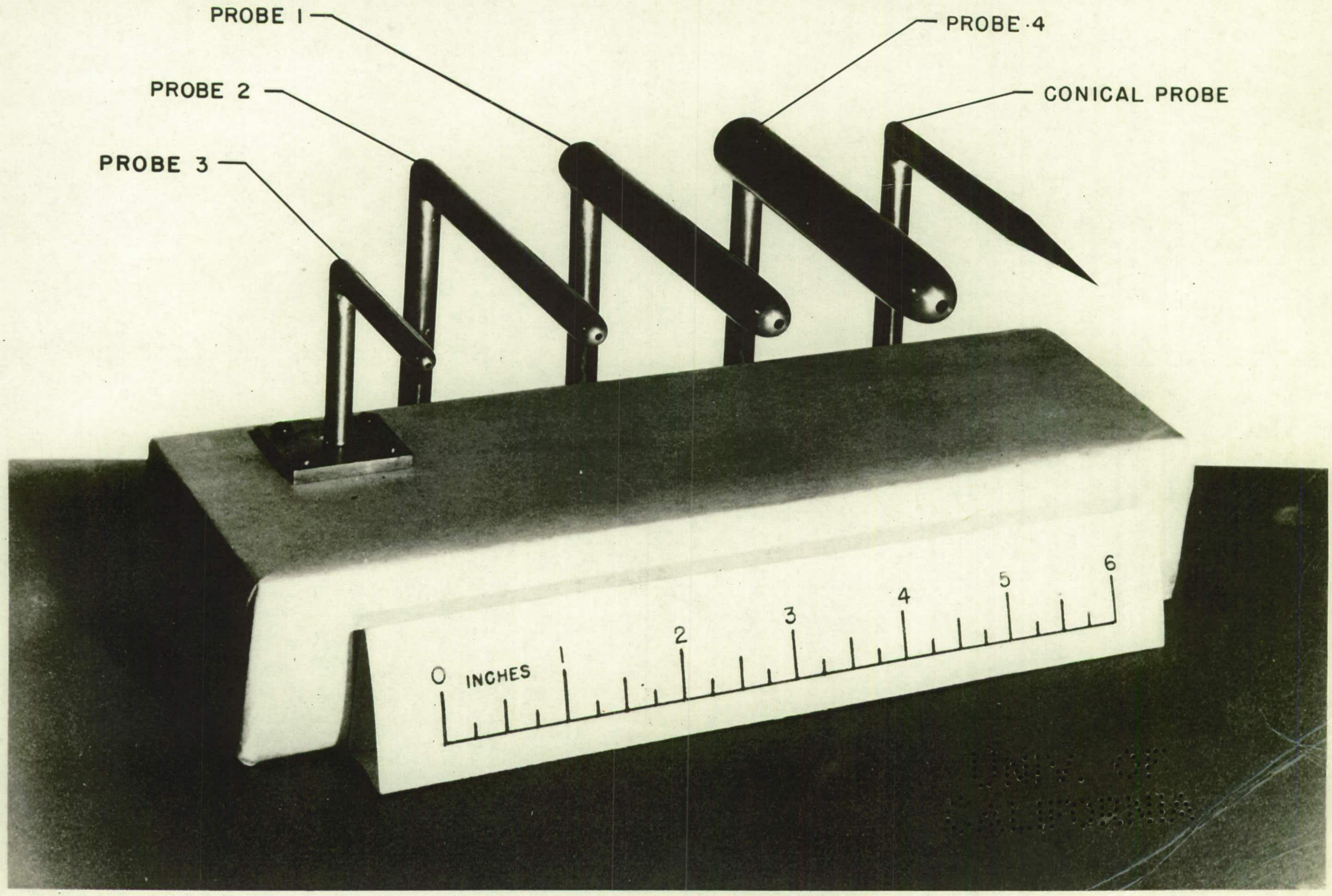

PHOTO 210

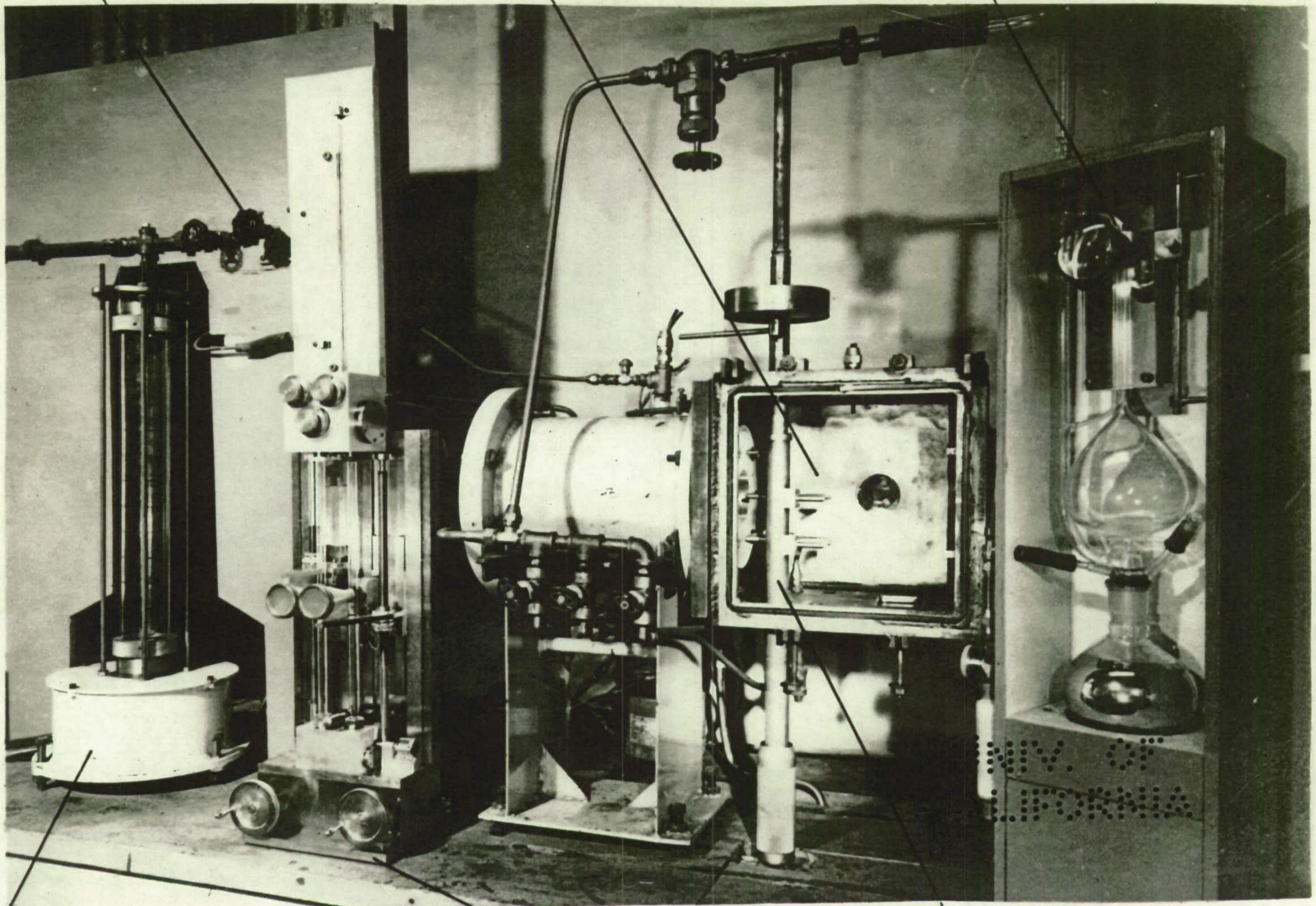
UPSTREAM VALVE
TEST SECTION
McLEOD GAGE
VOLUMETRIC FLOW METER
OIL MANOMETER
PROBE COLUMN

PHOTO 198